

INTRODUCTION

OpenFOAM is an open-source program based in C++ that can simulate incompressible and compressible fluid flows. Its complete list of pre-configured solvers, utilities and libraries makes it suitable for using in research or engineering applications. However, little attempt has been made to evaluate the different solvers and turbulence models in specific civil engineering applications such as river hydrodynamics, spillways or bridge piers. In order to validate one of the pre-configured turbulence models in OpenFOAM a comparison analysis was performed. The present work shows a comparison between three LES turbulence models: k-epsilon one equation model, Smagorinsky model and Spalart-Allmaras model. Herein, the case used was a duct with a mesh and boundary conditions explained in the following sections. Finally, the validation is performed by comparison with existing DNS data for a similar case.

METHODS

Mesh construction

To model the duct case mentioned in the introduction a hexahedral shape mesh was chosen. The dimensions of it are a height of 2m, a length of 4m and a width of 2m. The mesh was constructed using the program blockMesh included in the OpenFoam package. It is a structured mesh compound of hexahedral units. These units vary in the y axis from the center to the edges with a contraction factor of 0.1 (as shown in Figure 1) whereas the dimensions of every unit remains constant in the other two directions x and z. The latter is due to the need of a finer mesh in the top and bottom wall of the mesh. In that sense the duct is divided symmetrically by the red line shown in Figure 1 to allow the refining in the top and bottom walls. The resulting total number of faces was 184,700 and the number of points was 64,821.

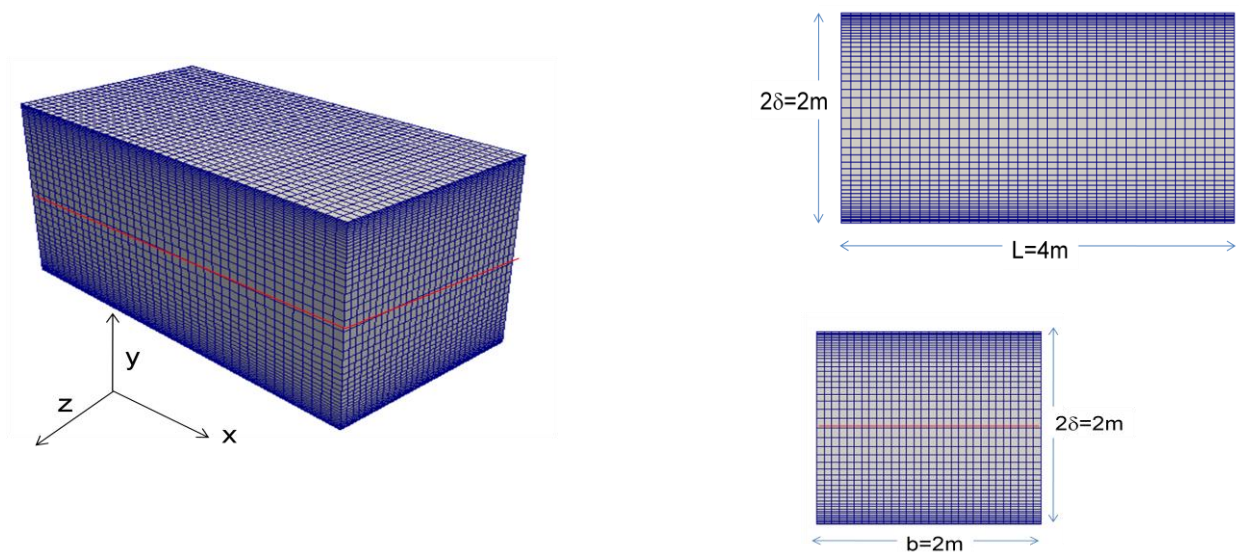


Figure 1-Duct Mesh using blockMesh

Boundary conditions

Figure 2 shows the boundary entities used in this case. To apply the initial boundary conditions to the domain the major faces of the mesh were named topwall, bottomwall, sides1, sides2 , inout1 and inout 2. The vertices are numbered considering a clockwise direction looking from the inside of the block to the outside. A list of the boundary faces is shown in Table 1.

Table 1-List of boundary faces

Face Name	Vertices
Topwall	(4 10 11 5)
Bottomwall	(0 1 7 6)
Sides1	(0 2 3 1) and (6 7 9 8)
Sides2	(2 4 5 3) and (8 9 11 10)
Inout1	(1 3 9 7) and (0 6 8 2)
Inout2	(3 5 11 9) and (2 8 10 4)

The entities called sides1, sides2; inout1 and inout2 were modeled with periodic boundary conditions making a continuous loop between them. For the internal velocity field a uniform initial value of 0.14 m/s was used. Whereas, for the initial velocity values at the walls fixed values of 0 were used. For the internal pressure field a uniform initial value of 0 was used. Additionally, the pressure was modeled considering a zero-gradient in the walls entities and periodic boundary conditions for the “sides” and “inout” entities.

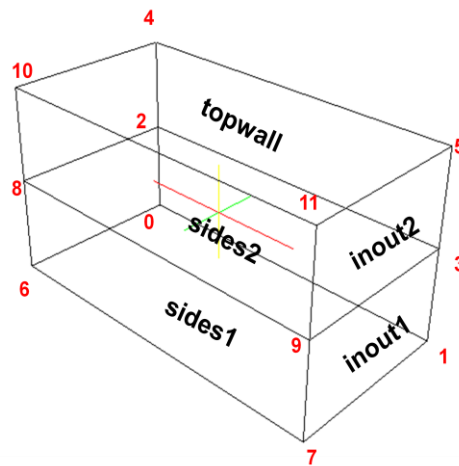


Figure 2-Boundary Entities

Equation Discretization

The time discretization was performed using a backwarding difference scheme. Converting the derivative time terms to integral terms we have that the linearized form of the backwarding difference scheme is given by:

$$\frac{\partial}{\partial t} \int_V \rho \phi dV = \frac{3(\rho_P \phi_P V)^n - 4(\rho_P \phi_P V)^o + 4(\rho_P \phi_P V)^{oo}}{2\Delta t}$$

Where the exponents n, o and oo represent the new values, old values and old-old values of the discretised term respectively. These values are given for ϕ by:

$$\phi^n = \phi(t + \Delta t)$$

$$\phi^o = \phi(t)$$

$$\phi^{oo} = \phi(t - \Delta t)$$

Additionally the variable ϕ represents any tensor field, ϕ_p represents any tensor field for the cell of interest P and the variable V represent the control volume. On the other hand the discretization for the gradient terms were linearized in integral form using Gauss theorem to the volume integral given by:

$$\int_V \nabla \phi dV = \int_S dS \phi = \sum_f S_f \phi_f$$

Where the subscript f is labeling the face of interest in a cell.

Results

The results of the simulation for the centerline of the middle section of the duct (shown in Figure 3) were compared with a DNS simulation performed by Kim et al (1987). The evaluated parameters were the mean velocity profile, the viscous stress and the Reynold stress. All the parameters were compared using a linear correlation coefficient R^2 and plotted against a normalized value of the distance given by y/δ . The mean velocity profile was generated using a normalized value by the bulk velocity defined as

$\bar{U} = \frac{1}{\delta} \int_0^\delta \langle U \rangle dy$ in which $\langle U \rangle$ represents de velocity time average. On the other hand, the viscous stress

was given by $\rho \nu \frac{d\langle U \rangle}{dy}$ in which ν represent the velocity fluctuation in the y direction. The Reynold

stress was given by $\rho \langle uv \rangle$ in which u represents the velocity fluctuation in the x direction. Thus, the total shear stress is the sum of the viscous stress and the Reynold stress. Figures 4, 5 and 6 show the

comparison between the calculated parameters for the three turbulence models introduced in a previous section and the data of the Kim DNS simulation.

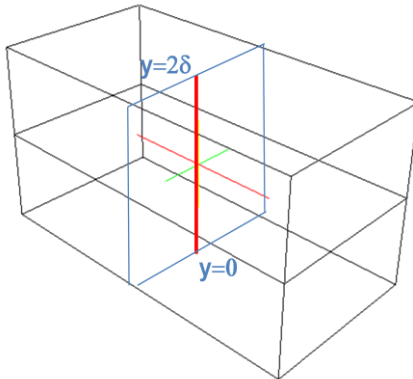


Figure 3-Centerline of Middle Section

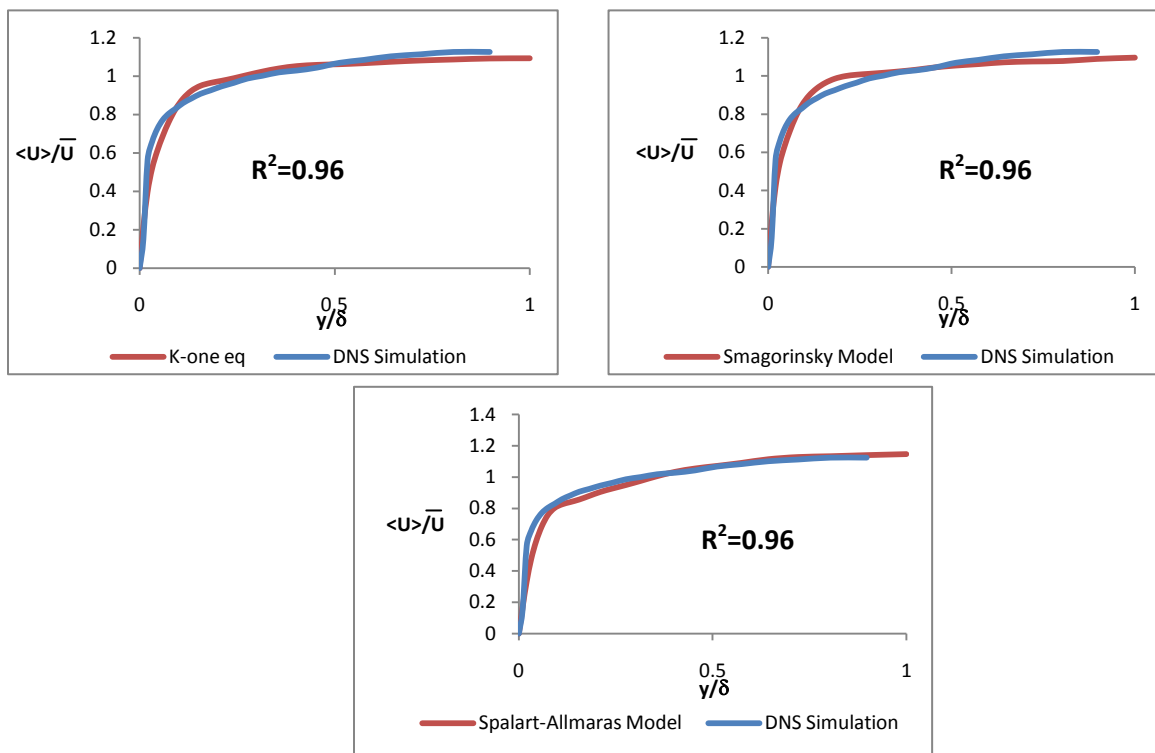


Figure 4-Velocity Mean Profiles for K-one eddy viscosity equation model, Smagorinsky Model, Spalart Allmaras Model and DNS Simulation

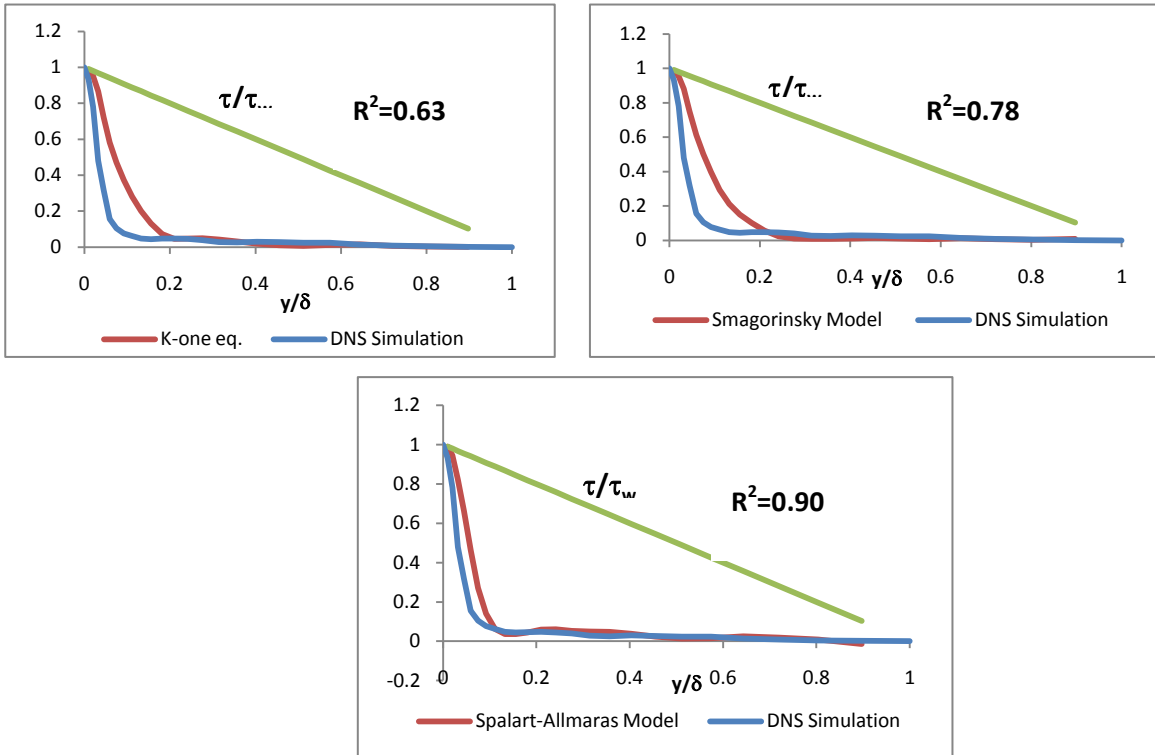


Figure 5-Viscous Stress for K-one eddy viscosity equation model, Smagorinsky Model, Spalart Allmaras Model and DNS Simulation

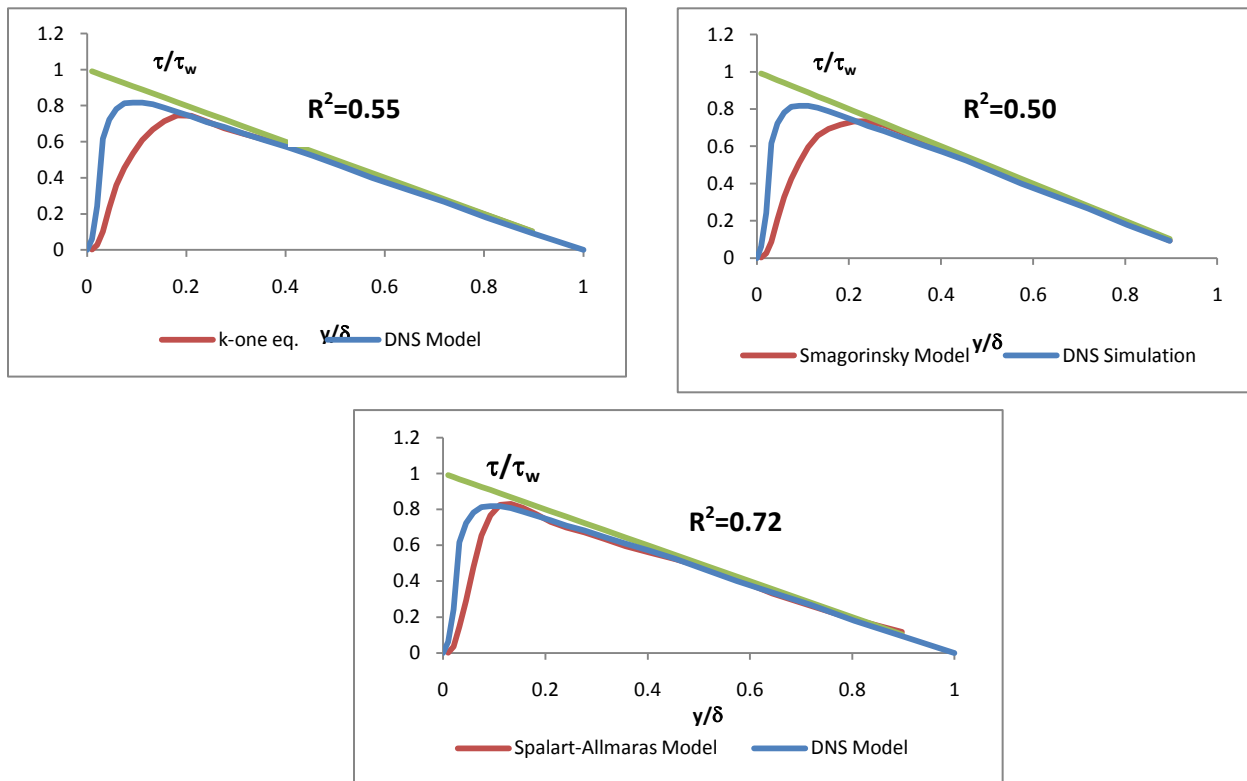


Figure 6-Reynold's Stress for K-one eddy viscosity equation model, Smagorinsky Model, Spalart Allmaras Model and DNS Simulation

DISCUSSION AND CONCLUSIONS

Although, all the turbulence models give the same level of correlation for the mean velocity profiles, visually the best correlated model is the Spalart-Allmaras as can be seen in Figure 4. According to Figure 4 the k-one equation eddy viscosity model and the Smagorinsky model trend to underestimate the values of velocity in the inner layer $y/\delta < 0.1$. Additionally, this models overestimates the velocity in the outer layer (in this case $y/\delta > 0.2$) up to the location $y/\delta=0.5$ where it starts to underestimate the velocity with an almost-horizontal slope curve.

In Figure 5, is shown that for the viscous stress parameter the Spalart-Allmaras model is the best correlated with a correlation coefficient of 0.90. However, the values of viscous stress are overestimate for the three turbulence models inside the inner layer. Additionally, in the Spalart-Allmaras model, after pass the inner layer the correlation improves in contrast to the other two models in where the viscous stress keep overestimate until a value of $y/\delta=0.2$

In Figure 6, is shown that for the Reynold's stress parameter the Spalart-Allmaras model is also the best correlated with a correlation coefficient of 0.72. Although this correlation coefficient represents that the model is not highly correlated with the DNS simulation is still a good reference value to consider the Spalart-Allmaras a good LES approximation in comparison with the two other models. In contrast to the behavior of the results for the viscous stress, the Reynold's stress is underestimating in the inner layer. The latter means that the expected correlation for the total shear stress will be better than the two separate components of it (viscous and Reynold's stress).

From the discussion above is concluded that the best LES turbulence model for the duct problem in OpenFOAM is the Spalart-Allmaras. The Spalart-Allmaras model (1994) is a one equation model developed for aerodynamics applications including boundary layer separation. The one equation model is given by:

$$\frac{\partial \tilde{v}}{\partial t} + u_j \frac{\partial \tilde{v}}{\partial x_j} = c_{b1}(1 - f_{t2})\tilde{S}\tilde{v} - \left[c_{w1}f_{w1} - \frac{c_{b1}}{\kappa^2}f_{t2} \right] \left(\frac{\tilde{v}}{d} \right)^2 + \frac{1}{\sigma} \left[\frac{\partial}{\partial x_j} \left((v + \tilde{v}) \frac{\partial \tilde{v}}{\partial x_j} \right) + c_{b2} \frac{\partial \tilde{v}}{\partial x_i} \frac{\partial \tilde{v}}{\partial x_i} \right]$$

Where the terms are defined by:

- Turbulent viscosity model: $\mu_t = \rho \tilde{v} f_{v1}$ with $f_{v1} = \frac{\chi^3}{\chi^3 + c_{v1}^3}$ and $\chi = \frac{\tilde{v}}{v}$.
- $\tilde{S} = \Omega + \frac{\tilde{v}}{\kappa^2 d^2} f_{v2}$, where Ω is the magnitude of vorticity, d is the distance from the field point to the nearest wall and $f_{v2} = 1 - \frac{\chi}{1 + \chi f_{v1}}$.
- $f_{w1} = g \left[\frac{1 + c_{w3}^6}{g^6 + c_{w3}^6} \right]^{1/6}$ where $g = r + c_{w2}(r^6 - r)$ and $r = \min \left[\frac{\tilde{v}}{S \kappa^2 d^2}, 10 \right]$.
- $f_{t2} = c_{t3} \exp \left(-c_{t4} \chi^2 \right)$.
- Finally the constants are: $c_{b1}=0.135$, $\sigma=2/3$, $c_{b2}=0.622$, $\kappa=0.41$, $c_{w2}=0.3$, $c_{w3}=2$, $c_{v1}=7.1$, $c_{t3}=1.2$, $c_{t4}=0.5$ and $c_{w1} = \frac{c_{b1}}{\kappa^2} + \frac{1+c_{b2}}{\sigma}$

REFERENCES

Abad, J. D., & Garcia, M. H. (2009). *Experiments in a high-amplitude Kinoshita meandering channel:1. Implications of bend orientation on mean and turbulent*. America Geophysical Union.

Constantinescu, G., Sukhodolov, A., & McCoy, A. (2009). *Mass exchange in a shallow channel flow with a series*. Environmental Fluid Mechanics Journal 9.

Hicks, F. E., Jin, Y. C., & Stefler, P. M. (1990). *Flow Near Sloped Bank in Curved Channel*. Journal of Hydraulic Engineering.

OpenCFD Limited. (2002). *OpenFOAM User Guide*. Boston: Free Software Foundation, Inc.

Pope, S. B. (2000). *Turbulent Flows*. Cambridge: University Press.

Shais, & Punzman. *Turbulence and Coherent Structures in Fluids, Plasmas and Nonlinear Media*.